HHS Public Access

Author manuscript

Cell Rep. Author manuscript; available in PMC 2016 March 09.

Published in final edited form as:

Cell Rep. 2016 February 9; 14(5): 991–999. doi:10.1016/j.celrep.2016.01.004.

Inborn Errors of Long Chain Fatty Acid β-Oxidation Link Neural Stem Cell Self-Renewal to Autism

Zhigang Xie[1,*], **Albert Jones**[2], **Jude T Deeney**[2], **Seong Kwon Hur**[1], and **Vytas A Bankaitis**[1]

[1]Department of Molecular and Cellular Medicine, Texas A&M University Health Science Center, College Station, TX 77843, USA

[2]Department of Medicine, Obesity Research Center, Boston University School of Medicine, Boston, MA 02118, USA

SUMMARY

Inborn errors of metabolism (IEMs) occur with high incidence in human populations. Especially prevalent among these are inborn deficiencies in fatty acid β-oxidation (FAO) clinically associated with developmental neuropsychiatric disorders, including autism. We now report that neural stem cell (NSC)-autonomous insufficiencies in activity of TMLHE (an autism-risk factor that supports long-chain FAO by catalyzing carnitine biosynthesis), of CPT1A (enzyme required for long-chain FAO transport into mitochondria), or of fatty acid mobilization from lipid droplets reduced NSC pools in mouse embryonic neocortex. Lineage tracing experiments demonstrated that reduced flux through the FAO pathway potentiated NSC symmetric differentiating divisions at the expense of self-renewing stem cell division modes. The collective data reveal a key role for FAO in controlling NSC-to-IPC transition in mammalian embryonic brain, and suggest NSC self-renewal as a cellular mechanism underlying the association between IEMs and autism.

INTRODUCTION

Inborn errors of metabolism (IEMs) affect circa 1 in every 800 live births in humans (Pampols, 2010), and are commonly associated with developmental brain syndromes such as autism spectrum disorders and cognitive disabilities. As those syndromes afflict ~1% and 2–3% of children, respectively (van Karnebeek and Stockler, 2012; Ghaziuddin and Al-Owain, 2013), these clinical associations argue that understanding the mechanisms underlying these associations will translate to major improvements in treating developmental brain diseases. However, little is known about such underlying mechanisms.

*Correspondence: zxie@tamhsc.edu.

Author Contributions. ZX conceptualized, designed, performed the research, analyzed the data, and wrote the manuscript. VAB designed the research, analyzed the data, and edited the manuscript. AJ and JTD designed, performed and analyzed FAO metabolic flux measurements. SKH contributed to in utero electroporation assays.

Deficiencies in mitochondrial FAO are particularly common IEMs. FAO pathways catabolize fatty acids of different chain lengths and represent a major metabolic engine for producing both ATP and reducing power (Houten and Wanders, 2010; Ito and Suda, 2014). The rate-limiting step for β-oxidation of long-chain fatty acids is their import from the cytoplasm into mitochondria (Figure S1A). This process requires carnitine as acyl carrier and the action of several enzymes -- including carnitine palmitoyltransferase I (CPT1) which catalyzes the rate-limiting reaction in this process. A distinct enzyme, the TMLHE trimethyllysine hydroxylase, executes the first step of carnitine biosynthesis (Strijbis et al., 2010). Interestingly, recent studies show that *TMLHE* mutations occur with high frequency in human populations (Celestino-Soper et al., 2012; Nava et al., 2012).

Previous studies of mitochondrial FAO largely focused on extracerebral tissues (Houten and Wanders, 2010). However, there is evidence to suggest an association between FAO deficiencies and developmental brain disorders such as autism. Autistic children present altered circulating levels of carnitine or acyl-carnitine – i.e., phenotypes suggestive of deficiencies in long-chain FAO (Clark-Taylor and Clark-Taylor, 2004; Filipek et al., 2004; Rossignol and Frye, 2011). Reciprocally, children identified as FAO-deficient by genetic screening commonly exhibit signature features of autism such as developmental delay (Waisbren et al., 2013). Finally, clinical associations of *TMLHE* mutations with increased autism risk are now established (Celestino-Soper et al., 2012; Nava et al., 2012). Yet, the underlying mechanisms underlying such associations remain unknown.

Given the growing recognition that intermediary metabolism is a central regulator of stem cell homeostasis (Ito and Suda, 2014), and that balanced NSC homeostasis is essential for proper brain development (Sun and Hevner, 2014; Taverna et al., 2014), we investigated whether the association between IEMs and developmental brain disorders has an NSC component. Herein, we report a direct involvement of long chain FAO in controlling the transition from NSCs to IPCs during brain development in embryonic mouse. The collective data make a strong case for deranged NSC homeostasis as a significant mechanistic foundation for interpreting the clinical associations between IEMs of fatty acid metabolism and neuropsychiatric disorders.

RESULTS

Reduced TMLHE Expression Causes Diminished NSC Pool in Embryonic Neocortex

The identification of *TMLHE* as an autism-risk gene motivated us to interrogate whether TMLHE regulates NSC homeostasis during development of the neocortex, the most recently evolved region of the mammalian brain and the one which houses higher brain functions. Both TMLHE transcript and protein were readily detected in mouse embryonic neocortex (Figures S1B,S1C). To determine whether and how TMLHE deficiencies affect NSCs, two independent shRNA plasmids for silencing *Tmlhe* expression were generated (Figures S1D,S1E). Adoption of loss-of-function strategies was motivated by reports that *TMLHE* mutations clinically associated with autism are expected to ablate, or strongly compromise, catalytic activity of this enzyme (Celestino-Soper et al., 2012; Nava et al., 2012). *Tmlhe*-directed shRNA plasmids were co-transfected with an EGFP plasmid into E12.5 murine neocortex by in utero electroporation. Embryos were returned to the uterus, allowed to

further develop, and were harvested at E15.5. The developmental fates of transfected $EGFP^+$ neocortical cells were subsequently followed by in situ immunostaining.

Mouse embryonic NSCs express the nuclear marker Pax6, and produce neurons primarily through IPCs that express the nuclear marker Tbr2 (Englund et al., 2005; Kowalczyk et al., 2009). Thus, $Pax6^+Tbr2^-$ cells were scored as NSCs and $Tbr2^+$ cells as IPCs. Nuclear markers were chosen over cytoplasmic NSC markers (e.g. Nestin) to assign cell identities because these enabled confident scoring of individual cells within the densely packed neocortical sections (Figure S1F). Quantifications based on Pax6 and Tbr2 nuclear marker labeling showed that embryonic neocortices electroporated with either of the *Tmlhe* shRNAs exhibited significant reductions in the fractional contribution of NSCs to total $EGFP^+$ cell populations (Figure 1).

TMLHE Catalytic Activity is Required For NSC Pool Maintenance

To ensure that the NSC phenotypes observed resulted from specific knockdown of TMLHE rather than off-target effects, a functional complementation experiment was performed. Whereas an shRNA-resistant wild-type TMLHE rescued the shRNA-induced NSC depletion in the in utero electroporation system, co-expression of the catalytic-dead $TMLHE^{D244H}$ did not (Figure 1). This non-functional mutant is the product of the autism-associated *TMLHE* c. 730G→C missense allele that alters D_{244} -- one of the three key residues of the TMLHE catalytic core (Monfregola et al., 2005). These data demonstrate that TMLHE catalytic activity is required for maintaining NSC pools in embryonic neocortex.

TMLHE-Deficiencies Preserve Key NSC Features

Several lines of evidence demonstrate *Tmlhe* shRNA challenges levied specific and biologically interesting NSC deficits. First, *Tmlhe* shRNA-induced reductions in the NSC pool were not due to enhanced cell death or apoptosis in the stem cell population as incidences of $EGFP^+$ cells exhibiting either fragmented nuclei or activated Caspase 3 were rare in control and *Tmlhe* shRNA groups (~0.1%; Figure S1G). Second, no obvious defects in neuronal migration or early neuronal differentiation were induced (Figures S1G,S1H). Third, TMLHE-deficiencies left intact other NSC properties critical for self-renewal. Sequential iododeoxyuridine (IdU)/chlorodeoxyuridine (CldU) injection experiments indicated TMLHE-deficiency did not alter length of NSC S-phase or cell cycle (Figures S2A–S2C). *Tmlhe* silencing also did not compromise nuclear migration to the ventricular surface of mitotic NSCs (Figures S2D,S2E) -- indicating that TMLHE-deficiency did not impair interkinetic nuclear migration. Similarly, no apparent defects were observed in NSC division cleavage plane (Figures S2F,S2G), or in the apical attachment (Figures S2H).

A BrdU labeling regimen, followed by analysis of actively cycling cells, showed *Tmlhe* shRNA challenge led to only a modest increase in cells exiting the cell cycle (Figures S2I,S2J). As the proliferating cell pool consists of both NSCs and IPCs, and given that most IPCs generate postmitotic neurons directly (most NSCs generate neurons via proliferating IPCs), this modest elevation in cell cycle exit was accounted for by the elevated contribution of IPCs to the proliferating population of *Tmlhe* shRNA-expressing cells.

CPT1-Deficiencies Compromise NSC Pools

To buttress the TMLHE knockdown/rescue results, we tested whether interference with an independent step in the mitochondrial long-chain FAO pathway similarly depleted NSC pools in embryonic neocortex. To that end, the rate-limiting enzyme for long-chain FAO (CPT1) was targeted for inhibition. Of the three CPT1 isoforms, CPT1A was so chosen because *Cpt1a* is expressed in embryonic neocortex -- particularly in the ventricular zone (Figure S3A; Genepaint ID: MH509). By contrast, CPT1C does not regulate mitochondrial FAO as a carnitine palmitoyltransferase (Wolfgang and Lane, 2011), and *Cpt1b* transcripts are not detected in embryonic mouse brain (Genepaint ID: EG2818).

As mice ablated for *Cpt1a* suffer an early uncharacterized embryonic lethality (Nyman et al., 2005), a *Cpt1a*-directed shRNA plasmid (Figure S3B) was co-electroporated with an EGFP plasmid into embryonic neocortex at E12.5 and embryos analyzed at E15.5. Indeed, *Cpt1a* shRNA challenge resulted in a significant decrease in the fractional representation of NSCs in $EGFP^+$ cell populations, and this NSC depletion was reversed upon co-expression of an shRNA-resistant *Cpt1a* cDNA (Figures 2A,2B). Moreover, as was observed for *TMLHE* deficiencies, CPT1A silencing neither enhanced apoptosis nor did it overtly compromise neuronal migration or differentiation (Figures S3C,S3D).

CPT1A involvement in regulating NSC homeostasis was similarly evident upon NSC intoxication with etomoxir, a small molecule inhibitor of the enzyme. Because of difficulties in controlling etomoxir exposure in vivo, E12.5 forebrain hemispheres were cultured in media with or without 100μM etomoxir – a concentration at which etomoxir inhibited FAO activity in neocortical cultures dominated by NSCs (Figures 2C,2D). The associated phenotypic consequences were thinning of the ventricular zone ($Pax6^+$ layer) with accompanying increases in $Pax6^+Tbr2^+$ IPC populations (Figures 2E,2F) – i.e. results congruent with the phenotypes evoked by *Tmlhe* and *Cpt1a* knockdown in intact neocortex. Taken together, the complementary gene silencing and pharmacological intervention data demonstrated that reduced metabolic flux through the long-chain FAO pathway upsets NSC homeostasis.

Reduced Fatty Acid Mobilization from Lipid Droplets Diminishes the NSC Pool

Lipid droplets (LDs) are primary fatty acid depots for mitochondrial FAO (Gross and Silver, 2014), and these structures are found in embryonic NSCs (Bush et al., 1992; Saito et al., 2009). To test whether interfering with fatty acid mobilization from LDs recapitulates the NSC derangements induced by direct compromise of mitochondrial FAO, a dominant-negative interference assay was developed. The experiment was grounded upon demonstrations that PLIN1 inhibits LD lipolysis by prohibiting lipase access to LD surfaces. Phosphorylation of PLIN1 by PKA at 6 sites releases this lipolytic block, and PLIN1 mutants that cannot be so phosphorylated are potent dominant-negative inhibitors of LD lipolysis (Figure S3E; Gross and Silver, 2014; Sztalryd and Kimmel, 2014). Co-electroporation of an EGFP plasmid with a vector driving expression of either a mutant PLIN1 with all 6 PKA phosphorylation sites mutated to alanine (PLIN1-6A), or a PLIN1 with 5 of the 6 PKA sites mutated to alanine (PLIN1-5A), evoked significant reductions in NSC pool size (Figures 2G,2H). Those effects were again evident in the absence of

enhanced cell death/apoptosis or overt defects in neuronal migration or neuronal differentiation (Figures S3F,S3G). The data show that withholding LD-derived fatty acids from an otherwise unadulterated mitochondrial FAO pathway elicits NSC homeostatic defects similar to those evoked by direct interference with activities of FAO enzymes.

FAO Regulates Mitochondrial Redox State

FAO is a major supply for both ATP and reducing power (Houten and Wanders, 2010; Ito and Suda, 2014). To address how diminutions in FAO metabolic flux affect these two NSC parameters, TMLHE and CPT1A expression were individually knocked-down by in utero electroporation. Relative ATP levels and redox state were then estimated by taking advantage of imaging readouts afforded by dedicated fluorescent biosensors. To those ends, a plasmid for expressing AT1.03, a cytoplasmic FRET-based ATP biosensor (Imamura et al., 2009), or a mitochondrial targeted AT1.03 (mtAT1.03), was co-electroporated with appropriate shRNA vectors into embryonic neocortex. Transfected cells exhibiting signature NSC morphologies (bipolar with an apical process contacting ventricular surface) and locations (soma close to ventricular surface) were analyzed by ratiometric YFP/CFP FRET imaging. No significant differences in FRET/CFP ratios were discerned between control and *Tmlhe* shRNA or *Cpt1a* shRNA groups (Figures S3H–S3K), reporting that NSCs maintained substantially normal bulk and mitochondrial ATP levels in the face of TMLHE or CPT1A deficiency.

To monitor mitochondrial redox status in transfected NSCs, a MitoTimer expression vector was co-electroporated with appropriate shRNA plasmids into E12.5 embryonic mouse neocortex. MitoTimer is a mitochondrial-targeted GFP whose emission wavelengths are sensitive to redox state of the environment (Laker et al., 2014). Analyses of MitoTimer fluorescence properties were again restricted to transfected cells with morphologies and tissue distributions diagnostic of NSCs. In those cells, MitoTimer localized correctly to mitochondria, and the punctate MitoTimer localization profiles were similar amongst all experimental groups (Figure S3L). Thus, neither *Tmlhe* nor *Cpt1a* deficiencies induced significant morphological derangements in the mitochondrial network. However, ratiometric analyses of MitoTimer green/red fluorescence emission spectra reported significant red shifts in NSCs expressing *Tmlhe* shRNA or *Cpt1a* shRNA relative to controls (Figures S3M,S3N) – indicating diminished flux through the FAO pathway resulted in oxidized NSC mitochondrial environments.

TMLHE Regulates NSC Daughter Cell Fate

Embryonic mouse NSCs undergo three exquisitely balanced modes of cell division: (i) a symmetric self-expanding mode that produces two NSC daughters, (ii) an asymmetric division that produces one NSC and one differentiated daughter, and (iii) a symmetric differentiating mode which produces two differentiated daughters. To assess whether TMLHE deficiency upsets the NSC division program, a two-step electroporation assay was performed to fate daughter pairs derived from the same NSC parent under conditions of reduced TMLHE expression (Figure S4A). In this assay, analyses focused exclusively on vicinal $EGFP^{+}mCherry^{+}$ cell pairs as these were inferred to represent daughters arising from one NSC parent.

In the control group, the majority of vicinal $EGFP^+mCherry^+$ cell pairs scored either as NSC/IPC or as NSC/NSC (Figures S4B,S4C), and only a minority scored as IPC/IPC (Figures 3A,3B). In the *Tmlhe* knockdown group, the incidences of both NSC/IPC and NSC/NSC cell pairs were decreased (Figures S4B,S4C) while the fractional contribution of IPC/IPC cell pairs was markedly increased (Figures 3A,3B). These data suggest that TMLHE maintained NSC pool integrity by inhibiting symmetric differentiating divisions that produce two IPCs.

The effect of TMLHE-deficiency on NSC daughter fate was recapitulated in a different assay, where Attractene, a nonliposomal transfection reagent, was used to transfect mouse embryonic neocortex *in vivo*. When an EGFP plasmid was co-injected with Attractene into lateral ventricles of E13.5 mouse embryos, EGFP expression was already apparent 10h after injection and became robust by 15h. In samples with low transfection efficiencies, $EGFP^+$ cells were scattered around the lateral ventricle as isolated single cells or cell pairs, which were interpreted to be derived from the division of transfected single cells. Immunostaining analysis at 15h after transfection revealed that all $EGFP^+$ cells (>300 cells examined) were either NSCs or IPCs. Moreover, most of the cell pairs (>90%) were either NSC/IPC or NSC/NSC pairs, while the remainder scored as IPC/IPC pairs (Figures S4D, S4E). As IPCs divide to produce IPCs or postmitotic neurons (but not NSCs), while NSCs divide to produce both NSCs and IPCs, these data indicated the Attractene regimen preferentially transfected NSCs.

To determine the effect of TMLHE-deficiency on daughter cell fate during NSC division, a mixture of EGFP plasmid and control or *Tmlhe* shRNA was co-injected with Attractene into the lateral ventricle of E13.5 mouse embryos, and cell fates of $EGFP^+$ cell pairs (but not $EGFP^+$ single cells or clones of >2 $EGFP^+$ cells) were analyzed after 24h when *Tmlhe* shRNA-induced NSC defects were already detectable (Figures S4F, S4G). *Tmlhe* shRNA challenge led to a dramatic increase in the fractional representation of IPC/IPC cell pairs, and this increase was again corrected by co-expression of silencing-resistant wild-type TMLHE, but not silencing-resistant $TMLHE^{D244H}$ (Figures 3C,3D). Both the fractional representation of NSC/IPC pairs and that of NSC/NSC pairs decreased in the *Tmlhe* shRNA group (Figures S4H,S4I). While the phenotypes in the Attractene experiments were somewhat milder than those in the two-step electroporation experiments, this difference was expected as it is the likely consequence of less efficient depletion of endogenous TMLHE protein in the Attractene regimen (the interval between shRNA transfection and cell fate analysis was shorter). Thus, the two-step electroporation and the Attractene transfection data converge to provide compelling evidence that TMLHE deficiencies promote symmetric differentiating NSC divisions that produce two IPCs at the expense of symmetric NSC/NSC and asymmetric NSC/IPC cell division modes that support stem cell self-renewal.

Exogenous Carnitine Rescues *Tmlhe* shRNA-Induced NSC Defects

As TMLHE generates a biodeliverable product (carnitine), it was of interest to assess whether depletion of NSCs from embryonic neocortex in the face of TMLHE deficiencies could be remediated by providing carnitine to the tissue. Control or *Tmlhe* shRNAs were co-electroporated with an EGFP plasmid into mouse embryonic neocortex at E12.5, and

electroporated embryos were allowed to develop in utero for a further 24h before being sacrificed. Forebrain hemispheres were then dissected and incubated in physiological glucose media with or without carnitine supplementation for 18h (Figure 4A). Under those conditions, *Tmlhe* shRNA induced a 2-fold decrease in the fractional representation of NSCs in $EGFP^+$ cell populations, and this reduction was rescued by inclusion of carnitine in the incubation medium (Figures 4B,4C). Thus, derangements in NSC pools caused by TMLHE deficiencies are carnitine remedial. While the NSC pool was not completely recovered, we note that *Tmlhe* shRNA had already reduced NSC pool size by 24h after electroporation (i.e. prior to carnitine supplementation; Figures S4F,S4G). Further analyses revealed that, while carnitine supplementation significantly enlarged the NSC pool in the *Tmlhe* shRNA group, it did not expand the NSC pool in the control group (Figure 4C). This result indicated exogenous carnitine modulates NSC pools only when endogenous carnitine biosynthesis is compromised.

DISCUSSION

Herein, we demonstrate a critical requirement for long-chain FAO in maintaining NSC homeostasis in mammalian embryonic neocortex. The key evidence includes gene silencing and chemical inhibition approaches that interfere with distinct enzymatic reactions in the mitochondrial FAO pathway, and dominant-negative approaches that restrict substrate entry into a biochemically uncompromised mitochondrial FAO pathway. These results demonstrate that reduced flux through this catabolic pathway directly disturbs NSC homeostasis by inappropriately enhancing transition of NSCs to IPC lineages. Our findings offer a novel mechanistic framework for interpreting the associations between FAO deficiencies and developmental brain disorders, and provide a biochemical basis for why *TMLHE* scores as an autism-linked gene.

Lineage tracing experiments demonstrate that an active FAO pathway supports NSC pool maintenance in embryonic neocortex by dampening the frequency of symmetric differentiating cell divisions that give rise to lineage-restricted cells (IPCs) at the expense of NSC self-renewal. The relevance of this activity to autism is underscored by growing evidence that established autism-linked genes or pathways are key regulators of NSC-to-IPC transition (Mutch et al., 2010; Saffary and Xie, 2011; Bian et al., 2013; Lv et al., 2013; Krumm et al., 2014; O'Roak et al., 2014). Our data further show that flux through the mitochondrial FAO pathway controls some metabolic trigger that regulates daughter cell fate during NSC division. The nature of this trigger remains unclear. While in vitro data suggest FAO maintains energy levels in adult SVZ neural stem and/or progenitor cells (Stoll et al., 2015), our in vivo experiments measured no significant derangements in bulk or mitochondrial ATP pools in FAO-deficient NSCs. However, as ATP levels are highly buffered in cells, we cannot discount the possibility that mitochondrial FAO insufficiencies are accompanied by compensatory metabolic adaptations that marshal other metabolic resources in support of bulk intracellular ATP. Such compensatory metabolic adaptations might be accompanied by wider pleiotropic effects which could influence daughter cell fate during NSC division.

With regard to redox status, enhanced oxidative environments were registered in NSC mitochondria with diminished FAO activity -- suggesting enhanced oxidative microenvironments impair NSC self-renewal in mouse embryonic neocortex. While reactive oxygen species are reported to regulate NSC self-renewal in adult mouse brain (Le Belle et al. 2011), in that case oxidative stress promoted NSC self-renewal rather than diminishing that capacity – i.e. the conclusion we arrive at here. Perhaps NSC self-renewal is differentially regulated as a function of magnitude of the oxidative stimulus. Alternatively, embryonic NSCs may fundamentally differ from adult brain NSCs in their metabolic wiring.

Why has a direct role for FAO in NSCs and brain development been largely ignored? First, classical studies of brain energy metabolism focused on neurons, glial cells, or the brain at the organ level (Belanger et al., 2011). As NSCs constitute only a small fraction of brain cells, NSC metabolic activity does not contribute significantly to the bulk averaging measurements that define many analyses. Second, characterization of NSC defects in animal models of FAO deficiencies are confounded by broader physiological consequences of these metabolic defects. For instance, mice ablated for *Cpt1a* suffer an early embryonic lethality presumed to reflect systemic metabolic failures (Nyman et al., 2005). Third, previous studies of NSC metabolism relied on dissociated NSC cultures. Those strategies, while convenient, ignore niche parameters that regulate NSC self-renewal. By contrast, the experimental paradigms used herein imposed TMLHE and CPT1A insufficiencies acutely, in situ, and in a manner restricted to defined subsets of cells within embryonic neocortex. Such manipulation of NSCs, in an authentic physiological context, exposed the critical role played by long-chain FAO in NSC self-renewal. While our analyses were restricted to mitochondrial β-oxidation of long-chain fatty acids, inherited deficiencies in medium- and short-chain FAO pathways are also recognized to predispose affected patients to developmental challenges (Waisbren et al., 2013). Our findings now raise the possibility that those diseases also reflect derangements in NSC homeostatic control.

Finally, linkage of NSC homeostatic mechanisms with IEMs of developmental brain disorders holds clinical implications. TMLHE-deficiencies represent the most frequent IEMs (Pampols, 2010; Celestino-Soper et al., 2012; Nava et al., 2012) and are associated with increased autism risk. The carnitine-rescue experiment suggests actionable prophylactic measures minimizing developmental brain deficits associated with TMLHE deficiencies. We forecast that elevation of fetal carnitine supply will prove an effective strategy for alleviating developmental brain deficits associated with inborn *TMLHE* mutations. The commercial availability of carnitine as nutritional supplement notwithstanding, this compound is not on the list of dietary supplements recommended by the FDA for pregnant women. We suggest genetic screening of prospective parents for *TMLHE* mutations, coupled with inclusion of carnitine as a dietary supplement upon initial diagnosis of pregnancy, promises health mental benefits for newborns otherwise at significant risk for developmental brain disorders.

EXPERIMENTAL PROCEDURES

Detailed experimental procedures are provided in SUPPLEMENTAL EXPERIMENTAL PROCEDURES.

Animals and In Utero Electroporation

Swiss Webster female mice were purchased from Taconic (Hudson, NY), Charles River Laboratories (Wilmington, MA), or Harlan Laboratories (Houston, TX). Mice were handled in accordance with NIH and institutional guidelines on the care and use of animals. In utero electroporation was performed as described (Saffary and Xie, 2011).

Tissue Preparation and Immunostaining

Electroporated mouse embryos were sacrificed by decapitation. Forebrain hemispheres were fixed in 2% paraformaldehyde (prepared in PBS) for 20–30min. Cryosections (30–40μm) were prepared from hemispheres and used for immunostaining.

Statistical Analysis

Statistical analysis was performed using GraphPad Prism software.

Supplementary Material

Refer to Web version on PubMed Central for supplementary material.

Acknowledgments

This work was supported by the Robert A. Welch Foundation (Award BE0017 to VAB) and grants from the National Institute of Health (1R21HD069857 to ZX and RO1GM112591 to VAB). JTD was supported by NIH grant R01DK035914. We thank C. Gonzales for technical assistance, F. B. Gertler for providing the pCAX-EGFP and pCAX-mCherry plasmids, and L. H. Tsai, I. Delalle, and R. B. Mouneimne for microscopy support. The Pax6 antibody developed by A. Kawakami was obtained from the Developmental Studies Hybridoma Bank, developed under the auspices of the National Institute of Child Health and Human Development, and maintained by the University of Iowa, Department of Biology, Iowa City, IA 52242.

References

1. Bélanger M, Allaman I, Magistretti PJ. Brain energy metabolism: focus on astrocyte-neuron metabolic cooperation. Cell Metab. 2011; 14:724–738. [PubMed: 22152301]
2. Bian S, Hong J, Li Q, Schebelle L, Pollock A, Knauss JL, Garg V, Sun T. MicroRNA cluster miR-17-92 regulates neural stem cell expansion and transition to intermediate progenitors in the developing mouse neocortex. Cell Rep. 2013; 3:1398–1406. [PubMed: 23623502]
3. Bush KT, Lee H, Nagele RG. Lipid droplets of neuroepithelial cells are a major calcium storage site during neural tube formation in chick and mouse embryos. Experientia. 1992; 48:516–519. [PubMed: 1601118]
4. Celestino-Soper PB, Violante S, Crawford EL, Luo R, Lionel AC, Delaby E, Cai G, Sadikovic B, Lee K, Lo C, et al. A common X-linked inborn error of carnitine biosynthesis may be a risk factor for nondysmorphic autism. Proc Natl Acad Sci U S A. 2012; 109:7974–7981. [PubMed: 22566635]
5. Clark-Taylor T, Clark-Taylor BE. Is autism a disorder of fatty acid metabolism? Possible dysfunction of mitochondrial beta-oxidation by long chain acyl-CoA dehydrogenase. Med Hypotheses. 2004; 62:970–975. [PubMed: 15142659]
6. Englund C, Fink A, Lau C, Pham D, Daza RA, Bulfone A, Kowalczyk T, Hevner RF. Pax6, Tbr2, and Tbr1 are expressed sequentially by radial glia, intermediate progenitor cells, and postmitotic neurons in developing neocortex. J Neurosci. 2005; 25:247–251. [PubMed: 15634788]
7. Filipek PA, Juranek J, Nguyen MT, Cummings C, Gargus JJ. Relative carnitine deficiency in autism. J Autism Dev Disord. 2004; 34:615–623. [PubMed: 15679182]
8. Ghaziuddin M, Al-Owain M. Autism spectrum disorders and inborn errors of metabolism: an update. Pediatr Neurol. 2013; 49:232–236. [PubMed: 23921282]

9. Gross DA, Silver DL. Cytosolic lipid droplets: from mechanisms of fat storage to disease. Crit Rev Biochem Mol Biol. 2014; 49:304–326. [PubMed: 25039762]
10. Houten SM, Wanders RJ. A general introduction to the biochemistry of mitochondrial fatty acid β-oxidation. J Inherit Metab Dis. 2010; 33:469–477. [PubMed: 20195903]
11. Imamura H, Nhat KP, Togawa H, Saito K, Iino R, Kato-Yamada Y, Nagai T, Noji H. Visualization of ATP levels inside single living cells with fluorescence resonance energy transfer-based genetically encoded indicators. Proc Natl Acad Sci U S A. 2009; 106:15651–15656. [PubMed: 19720993]
12. Ito K, Suda T. Metabolic requirements for the maintenance of self-renewing stem cells. Nat Rev Mol Cell Biol. 2014; 15:243–256. [PubMed: 24651542]
13. Kowalczyk T, Pontious A, Englund, Daza CRA, Bedogni, Hodge FR, Attardo A, Bell C, Huttner WB, Hevner RF. Intermediate neuronal progenitors (basal progenitors) produce pyramidal-projection neurons for all layers of cerebral cortex. Cereb Cortex. 2009; 19:2439–2450. [PubMed: 19168665]
14. Krumm N, O'Roak BJ, Shendure J, Eichler EE. A de novo convergence of autism genetics and molecular neuroscience. Trends Neurosci. 2014; 37:95–105. [PubMed: 24387789]
15. Laker RC, Xu P, Ryall KA, Sujkowski A, Kenwood BM, Chain KH, Zhang M, Royal MA, Hoehn KL, Driscoll M, et al. A novel MitoTimer reporter gene for mitochondrial content, structure, stress, and damage in vivo. J Biol Chem. 2014; 289:12005–12015. [PubMed: 24644293]
16. Le Belle JE, Orozco NM, Paucar AA, Saxe JP, Mottahedeh J, Pyle AD, Wu H, Kornblum HI. Proliferative neural stem cells have high endogenous ROS levels that regulate self-renewal and neurogenesis in a PI3K/Akt-dependant manner. Cell Stem Cell. 2011; 8:59–71. [PubMed: 21211782]
17. Lv JW, Cheng TL, Qiu ZL, Zhou WH. Role of the PTEN signaling pathway in autism spectrum disorder. Neurosci Bull. 2013; 29:773–778. [PubMed: 24136242]
18. Monfregola J, Cevenini A, Terracciano A, van Vlies N, Arbucci S, Wanders RJ, D'Urso M, Vaz FM, Ursini MV. Functional analysis of TMLH variants and definition of domains required for catalytic activity and mitochondrial targeting. J Cell Physiol. 2005; 204:839–847. [PubMed: 15754339]
19. Mutch CA, Schulte JD, Olson E, Chenn A. Beta-catenin signaling negatively regulates intermediate progenitor population numbers in the developing cortex. PLoS One. 2010; 5:e12376. [PubMed: 20811503]
20. Nava C, Lamari F, Héron D, Mignot C, Rastetter A, Keren B, Cohen D, Faudet A, Bouteiller D, Gilleron M, et al. Analysis of the chromosome X exome in patients with autism spectrum disorders identified novel candidate genes, including TMLHE. Transl Psychiatry. 2012; 2:e179. [PubMed: 23092983]
21. Nyman LR, Cox KB, Hoppel CL, Kerner J, Barnoski BL, Hamm DA, Tian L, Schoeb TR, Wood PA. Homozygous carnitine palmitoyltransferase 1a (liver isoform) deficiency is lethal in the mouse. Mol Genet Metab. 2005; 86:179–187. [PubMed: 16169268]
22. O'Roak BJ, Stessman HA, Boyle EA, Witherspoon KT, Martin B, Lee C, Vives L, Baker C, Hiatt JB, Nickerson DA, et al. Recurrent de novo mutations implicate novel genes underlying simplex autism risk. Nat Commun. 2014; 5:5595. [PubMed: 25418537]
23. Pampols T. Inherited metabolic rare disease. Adv Exp Med Biol. 2010; 686:397–431. [PubMed: 20824458]
24. Rossignol DA, Frye RE. Mitochondrial dysfunction in autism spectrum disorders: a systematic review and meta-analysis. Mol Psychiatry. 2011; 17:290–314. [PubMed: 21263444]
25. Saffary R, Xie Z. FMRP regulates the transition from radial glial cells to intermediate progenitor cells during neocortical development. J Neurosci. 2011; 31:1427–1439. [PubMed: 21273427]
26. Saito K, Dubreuil V, Arai Y, Wilsch-Bräuninger M, Schwudke D, Saher G, Miyata T, Breier G, Thiele C, Shevchenko A, et al. Ablation of cholesterol biosynthesis in neural stem cells increases their VEGF expression and angiogenesis but causes neuron apoptosis. Proc Natl Acad Sci U S A. 2009; 106:8350–8355. [PubMed: 19416849]

27. Stoll EA, Makin R, Sweet IR, Trevelyan AJ, Miwa S, Horner PJ, Turnbull DM. Neural stem cells in the adult subventricular zone oxidize fatty acids to produce energy and support neurogenic activity. Stem Cells. 2015; 33:2306–2319. [PubMed: 25919237]
28. Strijbis K, Vaz FM, Distel B. Enzymology of the carnitine biosynthesis pathway. IUBMB Life. 2010; 62:357–362. [PubMed: 20306513]
29. Sun T, Hevner RF. Growth and folding of the mammalian cerebral cortex: from molecules to malformations. Nat Rev Neurosci. 2014; 15:217–232. [PubMed: 24646670]
30. Sztalryd C, Kimmel AR. Perilipins: lipid droplet coat proteins adapted for tissue-specific energy storage and utilization, and lipid cytoprotection. Biochimie. 2014; 96:96–101. [PubMed: 24036367]
31. Taverna E, Götz M, Huttner WB. The cell biology of neurogenesis: toward an understanding of the development and evolution of the neocortex. Annu Rev Cell Dev Biol. 2014; 30:465–502. [PubMed: 25000993]
32. van Karnebeek CD, Stockler S. Treatable inborn errors of metabolism causing intellectual disability: a systematic literature review. Mol Genet Metab. 2012; 105:368–381. [PubMed: 22212131]
33. Waisbren SE, Landau Y, Wilson J, Vockley J. Neuropsychological outcomes in fatty acid oxidation disorders: 85 cases detected by newborn screening. Dev Disabil Res Rev. 2013; 17:260–268. [PubMed: 23798014]
34. Wolfgang MJ, Lane MD. Hypothalamic malonyl-CoA and CPT1c in the treatment of obesity. FEBS J. 2011; 278:552–558. [PubMed: 21199367]

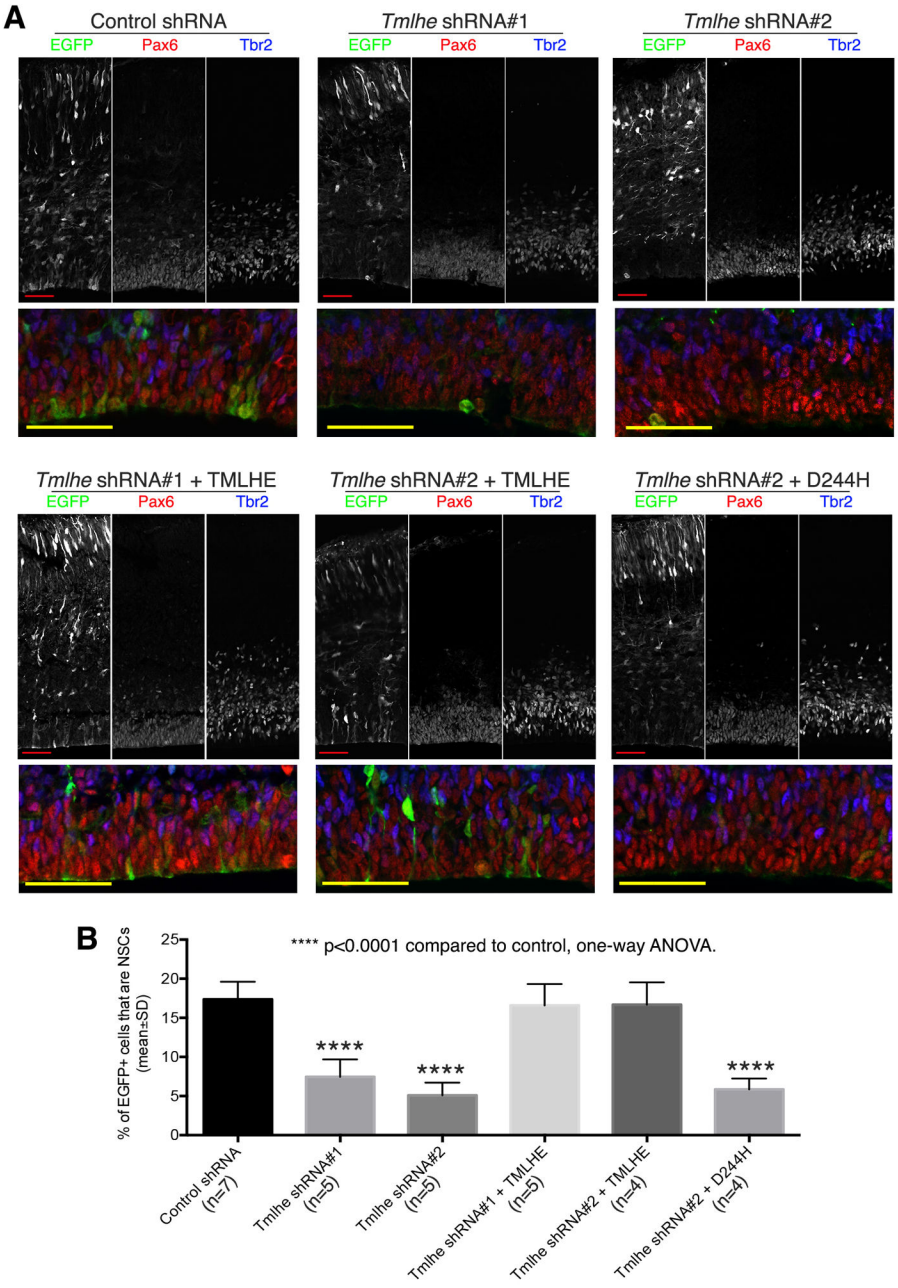

Figure 1. TMLHE Regulates the Size of NSC Pool in Mouse Embryonic Neocortex

Mouse embryos were co-electroporated with an EGFP plasmid and control or *Tmlhe* shRNA plasmid at E12.5, and sacrificed at E15.5. In rescue groups, a plasmid for expressing shRNA-resistant wild-type TMLHE (*Tmlhe* shRNA + TMLHE), or shRNA-resistant $TMLHE^{D244H}$ (*Tmlhe* shRNA + D244H), was co-electroporated with *Tmlhe* shRNA and EGFP plasmid. (A) Representative confocal images. Areas of the ventricular zone ($Pax6^{+}$ layer) are shown at higher magnification in bottom panels. (B) Quantification and statistics. Scale bars: 50μm. See also Figures S1 and S2.

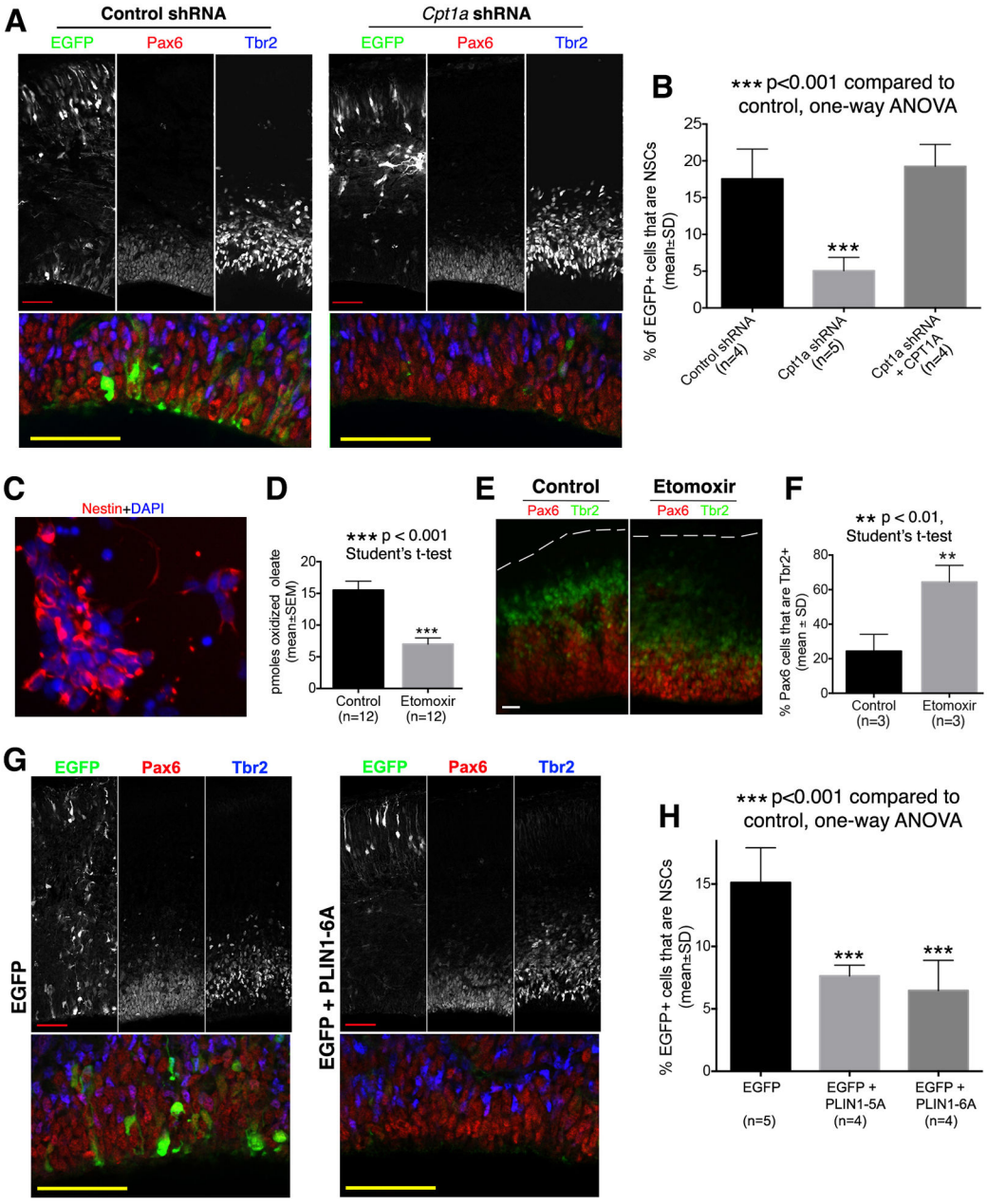

Figure 2. Targeting CPT1 or Fatty Acid Mobilization Diminished the NSC Pool

(A and B) Silencing *Cpt1a* diminished the NSC pool. Mouse embryos were electroporated at E12.5 and sacrificed at E15.5. In the rescue group (*Cpt1a* shRNA + CPT1A), a plasmid for expressing shRNA-resistant mouse *Cpt1a* cDNA was co-electroporated with *Cpt1a* shRNA and EGFP plasmid. (A) Representative confocal images. Areas of the ventricular zone ($Pax6^+$ layer) are shown at higher magnification in bottom panels. Scale bars: 50μm. (B) Quantifications. (C–F) Etomoxir induces increased differentiation of NSCs. (C) Neocortical cells used for FAO assay. Dissociated neocortical cells of E11.5 mouse embryos were cultured overnight, and then used in [^{14}C]-oleate oxidation assay for assessing FAO activity. Most cultured cells express the NSC marker Nestin. DAPI labels the nucleus of all cells.

Scale bar: 10μm. (D) [^{14}C]-Oleate oxidation assay confirms etomoxir inhibited FAO activity in cultured NSCs. (E and F) Etomoxir potentiated NSC differentiation in organotypic culture of forebrain hemispheres. (E) Representative images from three independent experiments showing reduced thickness of ventricular zone (Pax6$^+$ layer) in etomoxir group and increased fraction of Pax6$^+$ cells that co-express Tbr2. The pial surface is outlined by dashed lines. Scale bars: 20μm. (F) Quantifications. The percentage of Pax6$^+$ cells that co-express Tbr2 was significantly increased in the etomoxir group.

(G and H) Blocking fatty acid mobilization from lipid droplets by overexpressing dominant-negative mutants of PLIN1 diminished the NSC pool. Mouse embryos were electroporated at E12.5 and sacrificed at E15.5. (G) Representative confocal images. Areas of the ventricular zone (Pax6$^+$ layer) are shown at higher magnification in bottom panels. Scale bars: 50μm. (H) Quantification and statistics. See also Figure S3.

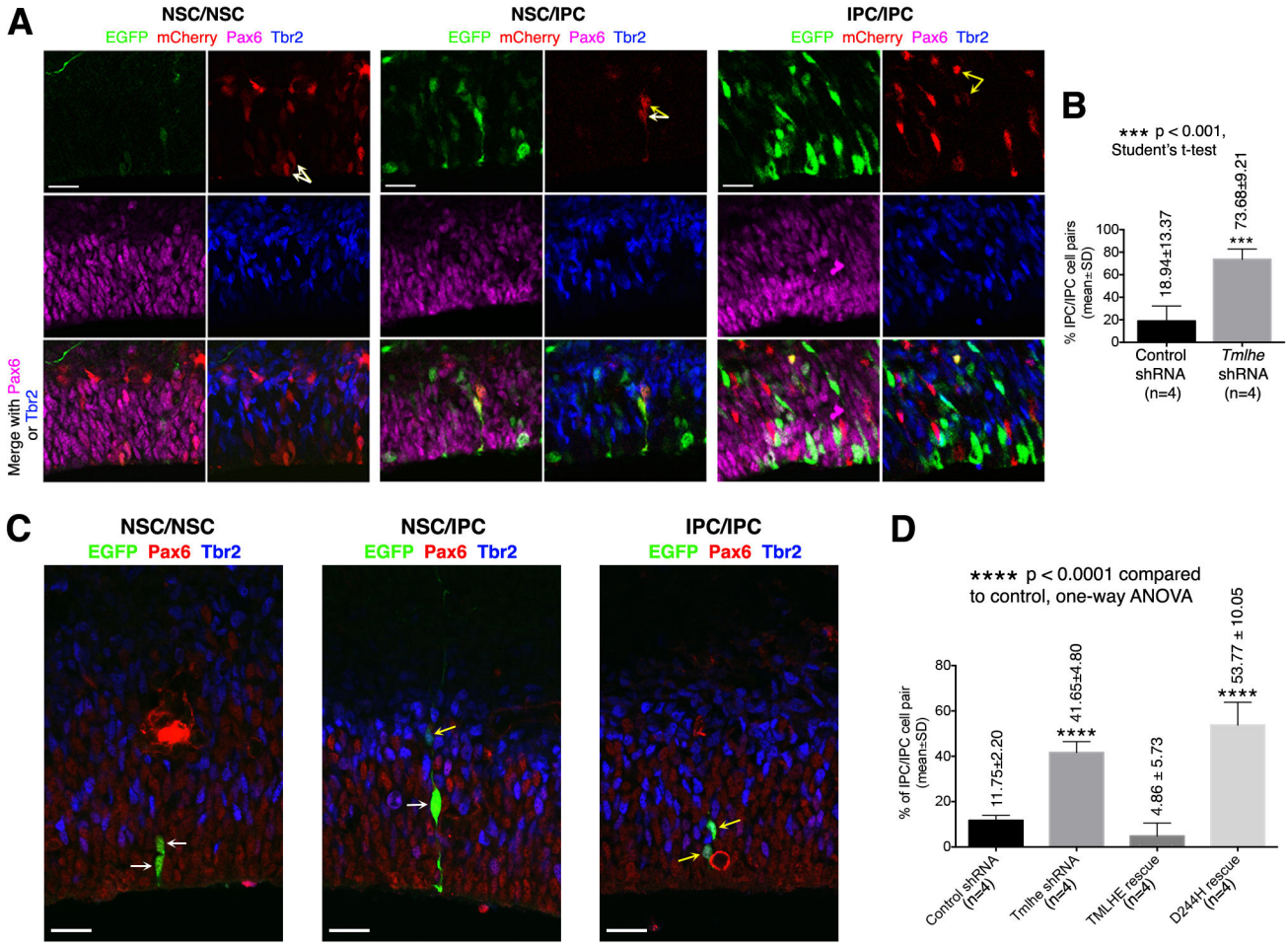

Figure 3. TMLHE Inhibits Symmetric NSC Division that Produces Two IPCs

(A and B) Analysis of NSC division by two-step electroporation assay. (A) Representative images showing vicinal EGFP$^+$mCherry$^+$ cell pairs of NSC/NSC, NSC/IPC, and IPC/IPC. White and yellow arrows indicate NSCs (Pax6$^+$Tbr2$^-$) and IPCs (Tbr2$^+$), respectively. Scale bars: 20μm. (B) Quantification and statistics. (C and D) Analysis of NSC division using Attractene-mediated transfection. (C) Representative images showing vicinal EGFP$^+$ cell pairs of NSC/NSC, NSC/IPC, and IPC/IPC. White and yellow arrows indicate NSCs and IPCs, respectively. Scale bars: 20μm. (D) Quantification and statistics. See also Figure S4.

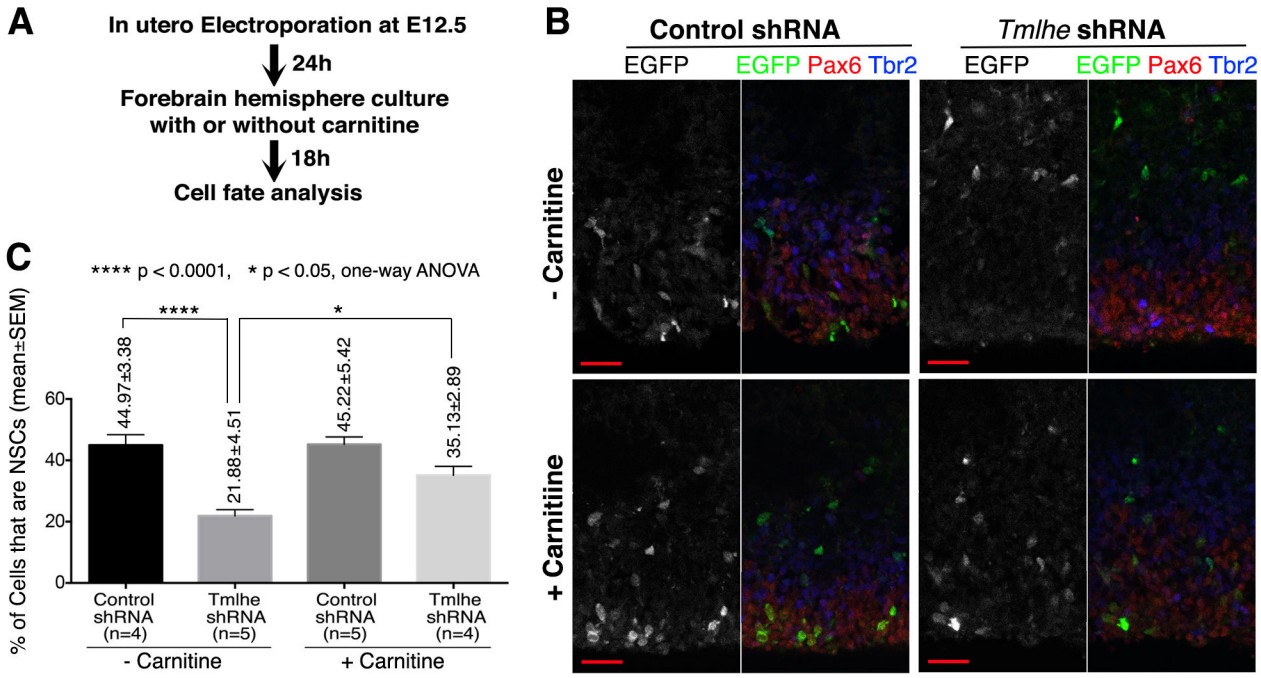

Figure 4. Exogenous Carnitine Largely Rescues *Tmlhe* shRNA-Induced NSC Defects

(A) Experimental procedures. (B) Representative confocal images. Scale bars: 20μm. (C) Quantification and statistics.